Supplemental Information - The Role of Stickiness in the Rheology of Semiflexible Polymers

Tom Golde,[1,2] Martin Glaser,[1,3] Cary Tutmarc,[1] Iman Elbalasy,[1]

Constantin Huster,[4] Gaizka Busteros,[1] David M. Smith,[3,1]

Harald Herrmann,[5,6] Josef A. Käs,[1] and Jörg Schnauß[1,3]

[1]*Peter Debye Institute for Soft Matter Physics,*
University of Leipzig, 04103 Leipzig, Germany
[2]*Institute for Bioengineering of Catalonia,*
The Barcelona Institute for Science and Technology, 08028 Barcelona, Spain
[3]*Fraunhofer Institute for Cell Therapy and Immunology, 04103 Leipzig, Germany*
[4]*Institute for Theoretical Physics, University of Leipzig, 04103 Leipzig, Germany*
[5]*Molecular Genetics, German Cancer Research Center, 69120 Heidelberg, Germany*
[6]*Department of Neuropathology, University Hospital Erlangen, 91054, Erlangen, Germany*
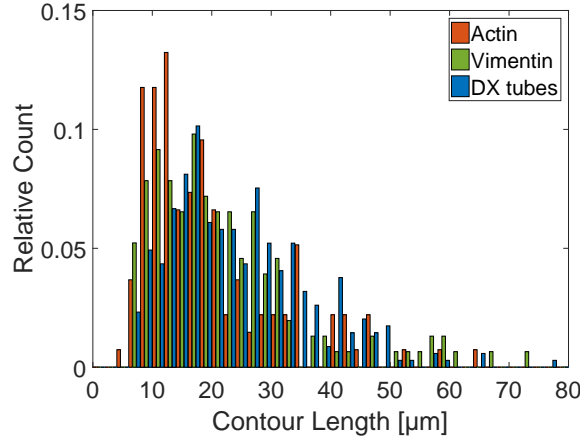
Figure S1. Histogram of the contour length L of F-actin ($n = 136$), vimentin IF ($n = 153$) and DX tubes ($n = 345$). Actin and vimentin data reproduced from [1].
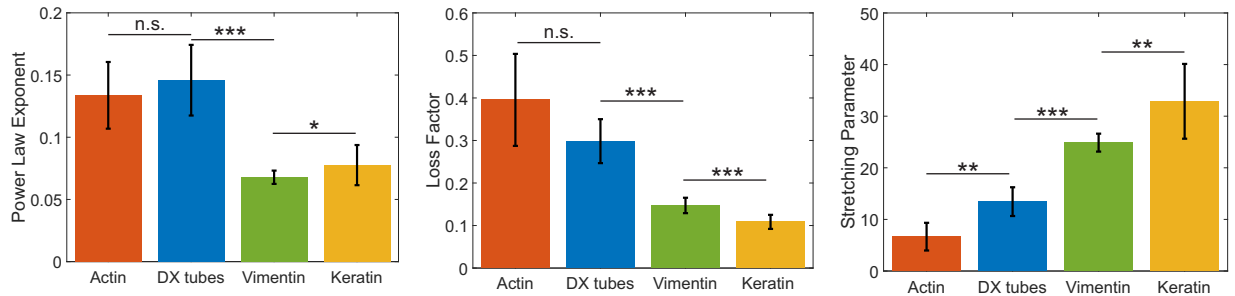
Figure S2. Local power law exponent α, loss factor $\tan(\phi)$ at a frequency $f = 1\,\text{Hz}$, and stretching parameter ε for F-actin, DX tubes, vimentin and keratin IF. Note that α and $\tan(\phi)$ are only approximations of the actual rheological properties. Differences of α and $\tan(\phi)$ are not significant for F-actin and DX tubes while both polymers behave significantly different to IF. ε combines both network properties and is significantly different for all four polymers. Each bar is the mean value of all samples with $n \geq 7$. Error bars are the standard deviation of the mean. Significance was tested with a Kolmogorow-Smirnow-test.
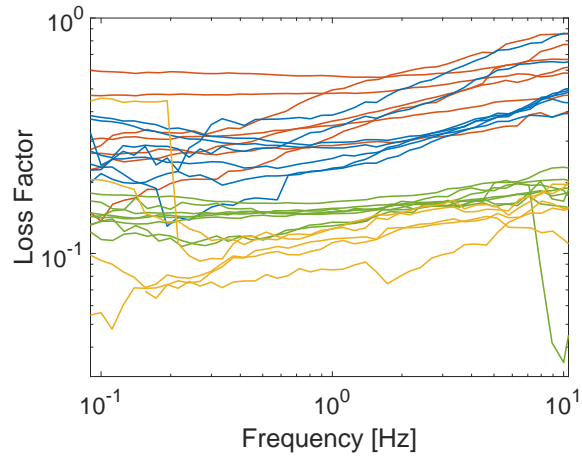
Figure S3. Loss factor $\tan(\phi)$ versus frequency for F-actin (red), DX tubes (blue), vimentin (green) and keratin (yellow) IF. Each line is a single measurement. Data has been smoothed with a moving average for better visibility.
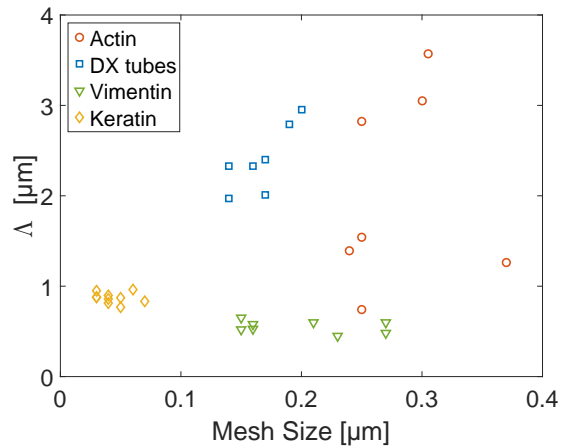
Figure S4. Interaction length Λ versus mesh size ξ. All values were obtained from fitting the complex shear modulus G^* of each sample to the GWLC.
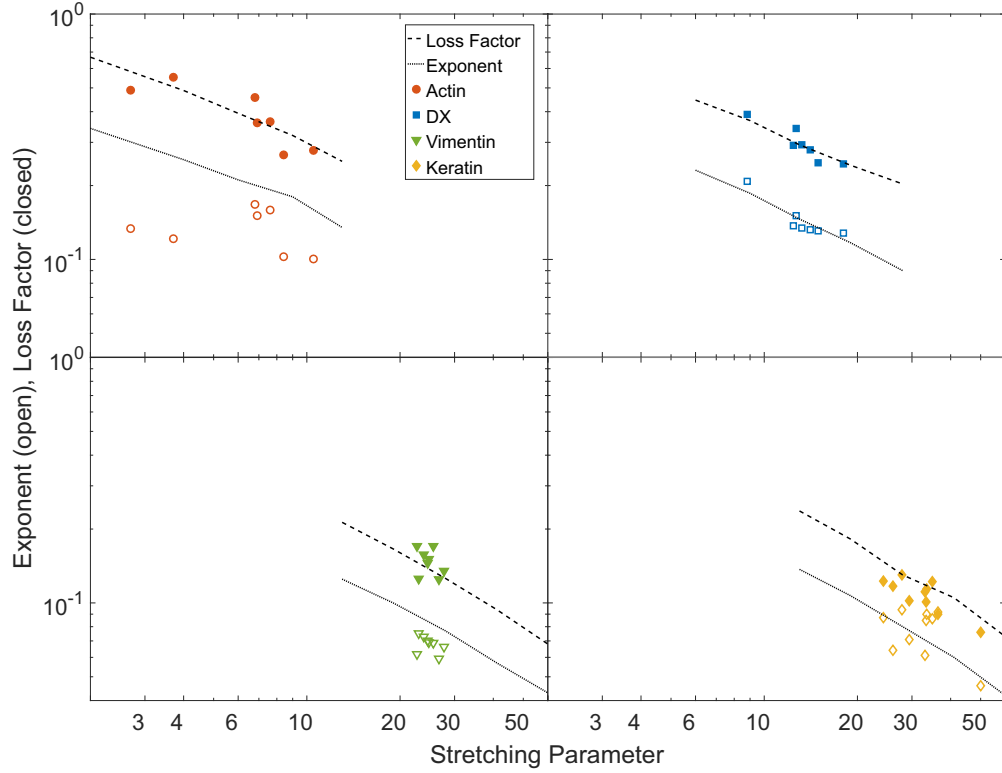
Figure S5. Local power law exponent of $G' \propto \omega^{\alpha}$ (open symbols) and loss factor $\tan(\phi) = G''/G'$ (solid symbols) versus stretching parameter ε. Each pair of data points represents one sample. The exponent was obtained from fitting G' with a power law for frequencies smaller than the cross-over between G' and G''. The loss factor was obtained from fitting $\tan(\phi)$ locally with a power law at a frequency of 1 Hz. ε is the result from fitting the complex shear modulus G^* to Eq.(3) for each sample. Dashed lines are the numerical results of an exemplary G^*_{GWLC} where all parameters except ε are fixed to the mean values of the polymer.
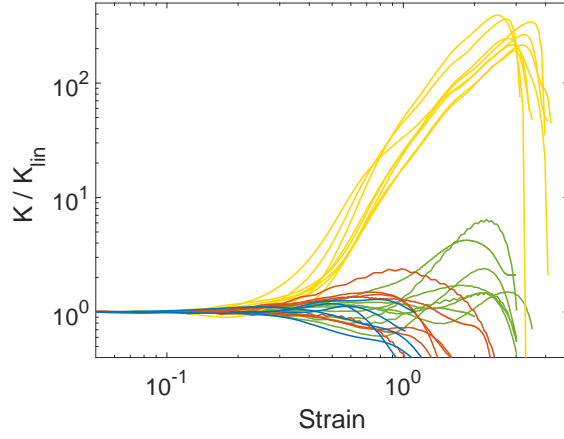
Figure S6. Differential shear modulus K rescaled by its value in the linear regime K_{lin} versus strain. Solid lines are single measurements of F-actin (red), DX tubes (blue) vimentin (green) and keratin (yellow) IFs samples. Actin and vimentin data reproduced from [1].
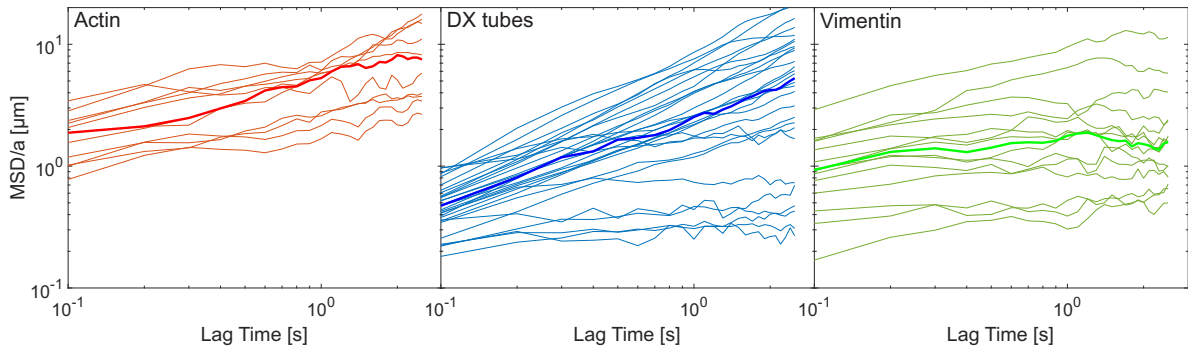
Figure S7. MSD of the filament center parallel to the tube rescaled by tube width a versus lag time τ. Thin lines are single filaments. Thick lines are the median over all presented filaments. Actin and vimentin data reproduced from [1].

SUPPLEMENTARY TABLES

linear rheology:		
contour length actin	L	16 µm [1]
contour length DX tubes	L	21 µm
contour length vimentin	L	18 µm [1]
contour length keratin	L	18 µm
contour length GWLC example	L	18 µm
persistence length actin	l_p	9 µm [2]
persistence length DX tubes	l_p	4 µm [3]
persistence length vimentin	l_p	2 µm [4, 5]
persistence length keratin	l_p	0.5 µm [6, 7]
persistence length GWLC example	l_p	4 µm
mesh size GWLC example	ξ	0.2 µm
interaction length GWLC example	Λ	1 µm
drag coefficient per length	$\zeta_\perp$	2 mPa s
non-linear rheology:		
characteristic width of a free energy well actin	δ	150 nm
characteristic width of a free energy well DX tubes	δ	2000 nm
characteristic width of a free energy well vimentin	δ	50 nm
characteristic width of a free energy well keratin	δ	50 nm
energy difference between the bound and the unbound state	U	2.5 $k_\mathrm{B}T$
control parameter for filament lengthening	S	0.13
distance between bound and unbound state	Δx	200 nm

Table SI. Fixed parameters for the description of the linear rheology and adjusted parameters for reproducing the non-linear rheology.

Name	Sequence
SE1	CTCAGTGGACAGCCGTTCTGGAGCGTTGGACGAAACT
SE2	GTCTGGTAGAGCACCACTGAGAGGTA
SE3	CCAGAACGGCTGTGGCTAAACAGTAACCGAAGCACCAACGCT
SE3-Cy3	CCAGAACGGCTGTGGCTAAACAGTAACCGAAGCACCAACGCTTT-Cy3
SE4	CAGACAGTTTCGTGGTCATCGTACCT
SE5	CGATGACCTGCTTCGGTTACTGTTTAGCCTGCTCTAC

Table SII. Sequences of the DNA oligonucleotides.

SI TEXT

The glassy wormlike chain model

The specific GWLC used for this study has been comprehensively described previously [1, 8, 9]. In general, the GWLC is an extension of the wormlike chain (WLC) for semiflexible polymer networks that takes into account the interactions of a test chain with its environment by stretching the mode relaxation spectrum of the WLC exponentially. Starting with the mode relaxation times of all eigenmodes of (half-) wavelength $\lambda_n = L/n$ and mode number n for a WLC with persistence length l_p and the transverse drag coefficient $\zeta_\perp$:

$$\tau_n^{\mathrm{WLC}} = \zeta_\perp/(l_\mathrm{p} k_\mathrm{B} T \pi^4/\lambda_n^4 + f\pi^2/\lambda_n^2), \tag{1}$$

the relaxation times of the GWLC are modified according to:

$$\tau_n^{\mathrm{GWLC}} = \begin{cases} \tau_n^{\mathrm{WLC}} & \text{if } \lambda_n \leq \Lambda \\ \tau_n^{\mathrm{WLC}} \mathrm{e}^{\varepsilon N_n} & \text{if } \lambda_n > \Lambda. \end{cases} \tag{2}$$

Here, $N_n = \lambda_n/\Lambda - 1$ is the number of interactions per length λ_n, L the contour length of the test filament, Λ the typical distance between two interactions, and f describes a homogeneous backbone tension accounting for existing pre-stress. ε is the stretching parameter controlling how strong the modes are slowed down by interactions with the environment. The complex linear shear modulus in the high frequency regime is then:

$$G^*(\omega) = \Lambda/(5\xi^2 \chi(\omega)), \tag{3}$$

with the mesh size ξ. $\chi(\omega)$ is the micro-rheological, linear response function to a point force at the ends of the GWLC:

$$\chi(\omega) = \frac{L^4}{\pi^4 l_{\mathrm{p}}^2 k_{\mathrm{B}} T} \sum_{n=1}^{\infty} \frac{1}{\left(n^4 + n^2 f/f_{\mathrm{E}}\right)\left(1 + i\omega\tau_n^{\mathrm{GWLC}}/2\right)}. \tag{4}$$

Here, $f_{\mathrm{E}} = l_{\mathrm{p}} k_{\mathrm{B}} T \pi^2 / L^2$ is the Euler buckling force. f is set to zero for the linear regime.

In the non-linear regime, the differential shear modulus $K = d\sigma/d\gamma$ is approximated via Eq.(3) at a constant frequency as a function of the backbone tension f:

$$K(f) = |G_{\omega}^{*}|(f), \tag{5}$$

where f is related to the macroscopic stress σ via $f = 5\sigma\xi^2$. The effect of pre-stress on the stretching parameter is introduced via a linear barrier height reduction:

$$\varepsilon \to \varepsilon - f\delta/k_{\mathrm{B}}T, \tag{6}$$

where δ should be interpreted as an effective width of a free energy well. The mean values of ξ, Λ and ε obtained from fitting the linear regime for each polymer type were used to replicate the measured curves. δ was used as the only free parameter to effectively shift the peak of K both in terms of σ and the maximum value $K_{\max}$.

An important question is how the other parameters are related to bottom up physical properties. The contour length L, for example, is naturally a broad distribution instead of a single value (Fig. S1). Different shapes and widths of this distribution might influence the network properties in a way that cannot be captured by a single number.

The mesh size ξ is rather an effective concentration scaling than the actual distance between neighboring filaments, although it has the right order of magnitude. The pre-factor in Eq.(3) originates from a purely geometric definition of the mesh. A quantitative matching of ξ with rheological data has been proven to be difficult for both F-actin and IF [7, 10].

The interaction length Λ is the average contour length between two sticky interactions of a test polymer. Thus, it is considered as a smeared out version of the entanglement length L_e in the original paper by Kroy and Glaser [8] although the GWLC is fundamentally different to the picture of a coarse grained tube. A strict identification of both appears to be too simple and the physical nature of Λ is still a matter of debate. In the tube model, L_e has a simple scaling of the form $L_e \propto l_p^{1/5}\xi^{4/5}$ [11] while more advanced approaches lead to slightly different exponents [12]. As expected, we cannot observe a systematic scaling of Λ with

either persistence length l_p or with mesh size ξ (Fig. S4). Its consistency for DX tubes and vimentin and keratin IF might contain some information about polymer specific interactions while the strong variation of Λ for F-actin is a direct consequence of the sample to sample variation of the cross-over frequency ω_Λ. The final interpretation of the interaction length Λ remains an important task for future investigations due to its strong influence on the transition between single polymer and interaction dominated network properties.

SUPPORTING REFERENCES

[1] T. Golde, C. Huster, M. Glaser, T. Händler, H. Herrmann, J. A. Käs, and J. Schnauß, Soft Matter **14**, 7970 (2018).

[2] H. Isambert, P. Venier, A. C. Maggs, A. Fattoum, R. Kassab, D. Pantaloni, and M. F. Carlier, J. Biol. Chem. **270**, 11437 (1995).

[3] P. W. K. Rothemund, A. Ekani-Nkodo, N. Papadakis, A. Kumar, D. K. Fygenson, and E. Winfree, J. Am. Chem. Soc. **126**, 16344 (2004).

[4] N. Mücke, L. Kreplak, R. Kirmse, T. Wedig, H. Herrmann, U. Aebi, and J. Langowski, J. Mol. Biol. **335**, 1241 (2004).

[5] B. Nöding and S. Köster, Phys. Rev. Lett. **108**, 088101 (2012).

[6] T. Lichtenstern, N. Mücke, U. Aebi, M. Mauermann, and H. Herrmann, J. Struct. Biol. Ueli Aebi Festschrift, **177**, 54 (2012).

[7] P. Pawelzyk, N. Mücke, H. Herrmann, and N. Willenbacher, PLoS ONE **9**, e93194 (2014).

[8] K. Kroy and J. Glaser, New J. Phys. **9**, 416 (2007).

[9] C. Semmrich, T. Storz, J. Glaser, R. Merkel, A. R. Bausch, and K. Kroy, PNAS **104**, 20199 (2007).

[10] D. C. Morse, Macromolecules **31**, 7044 (1998).

[11] D. C. Morse, Phys. Rev. E **58**, R1237 (1998).

[12] D. C. Morse, Phys. Rev. E **63**, 031502 (2001).